Supplemental Figure 1

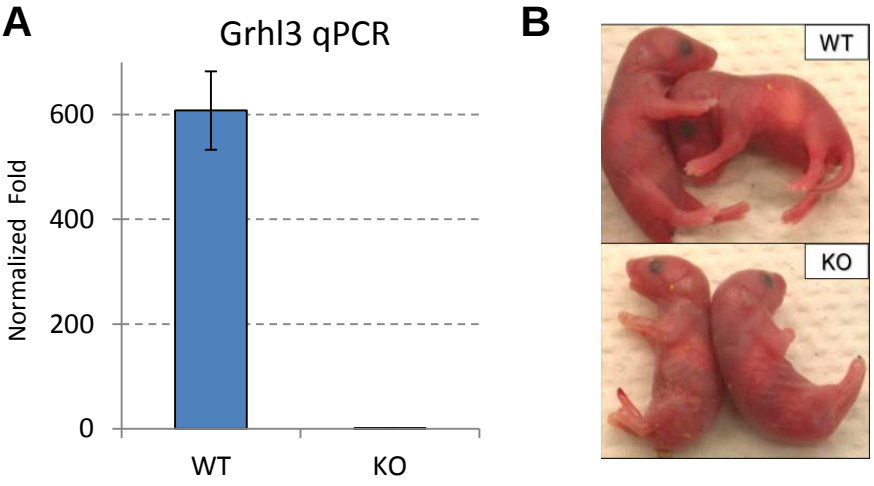

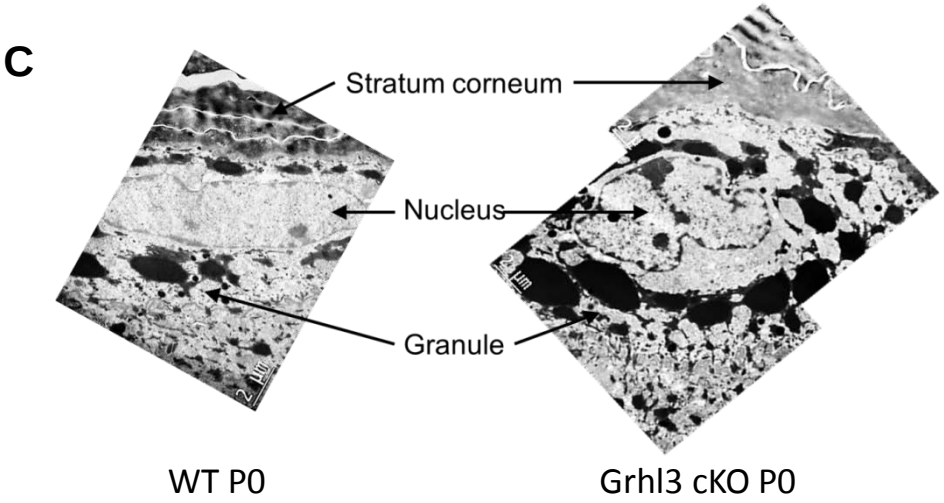

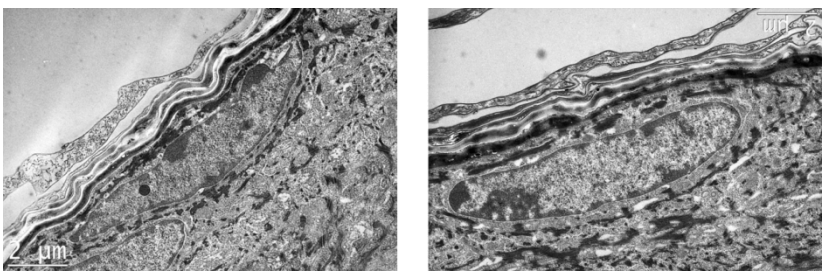

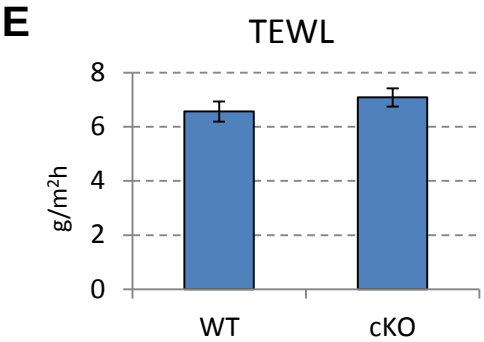

F

	Aox4	Krt6	Lor	Tgm1
P0 KO	-2.8	+2.3	-1.6	-2.1
P0 cKO	-2.2	+1.9	-1.8	-1.75
P56 cKO	-1.9	+2.5	-3.7	-1.5

Supplemental Figure 2

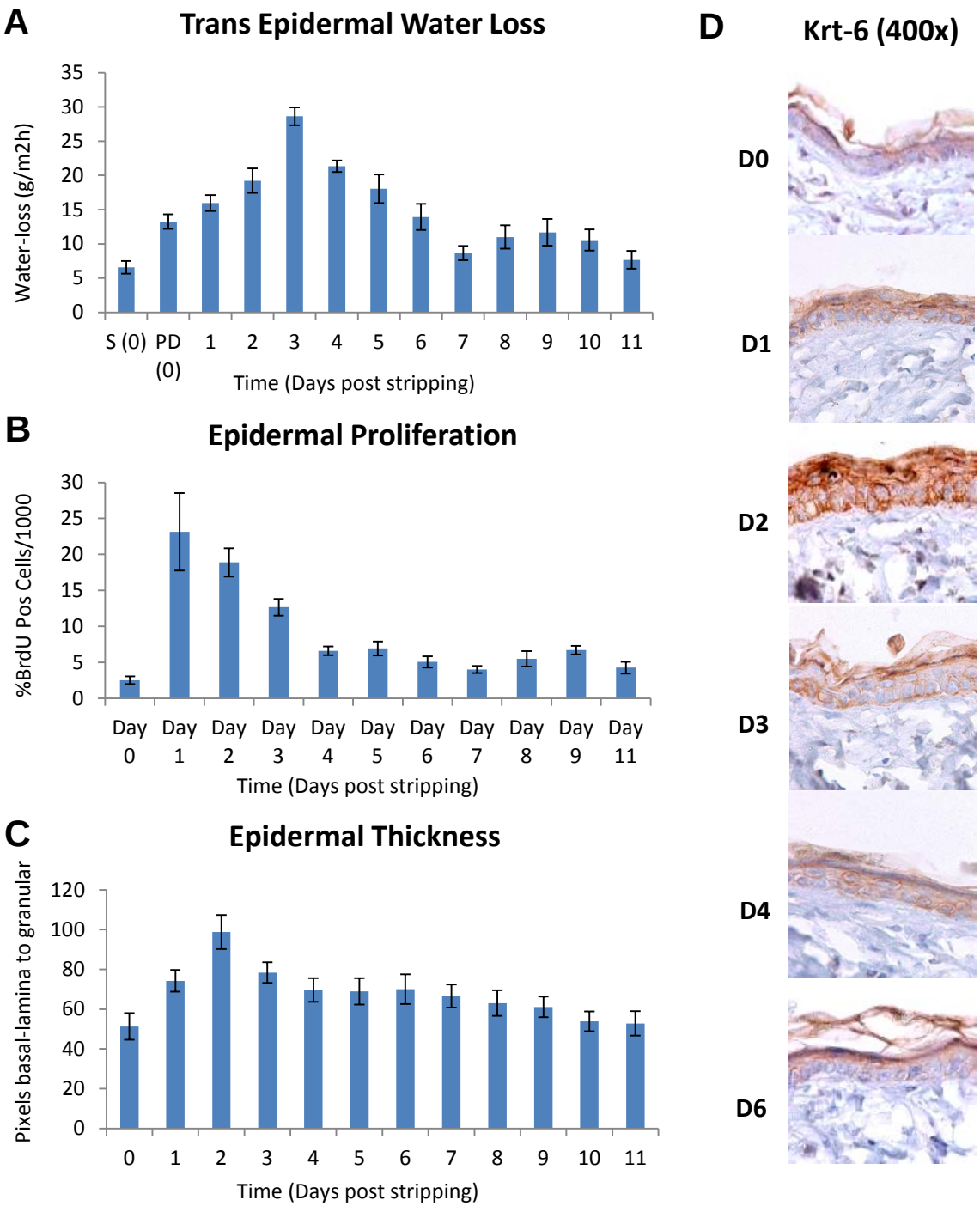

Supplemental Figure 3

A

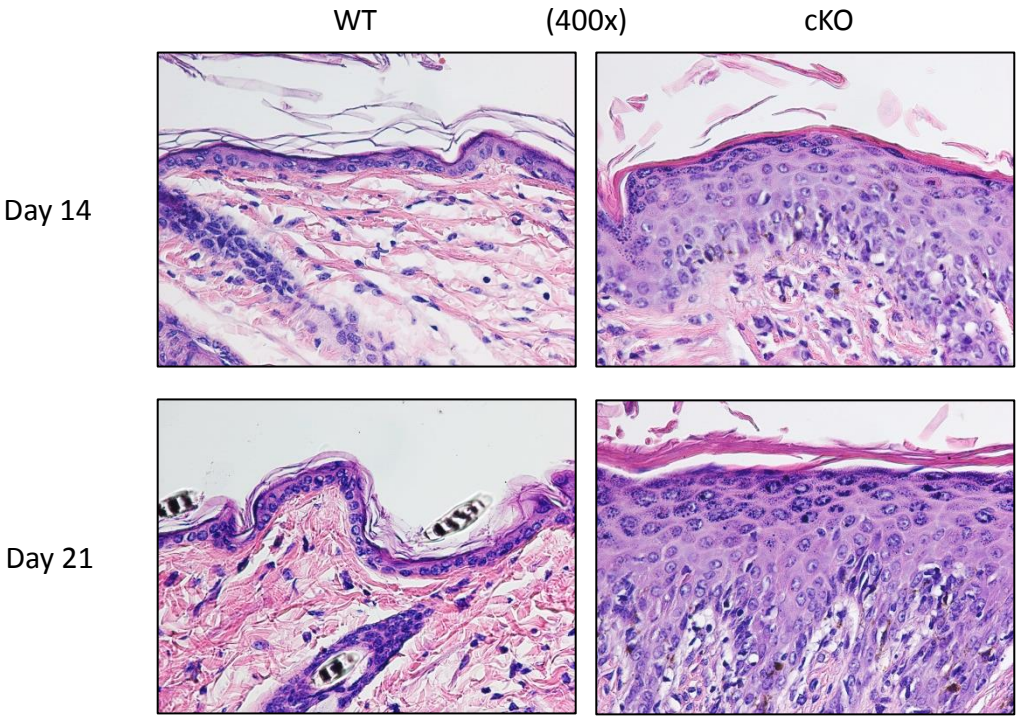

Wax Stripping Recovery for 14 and 21 days (H&E)

B

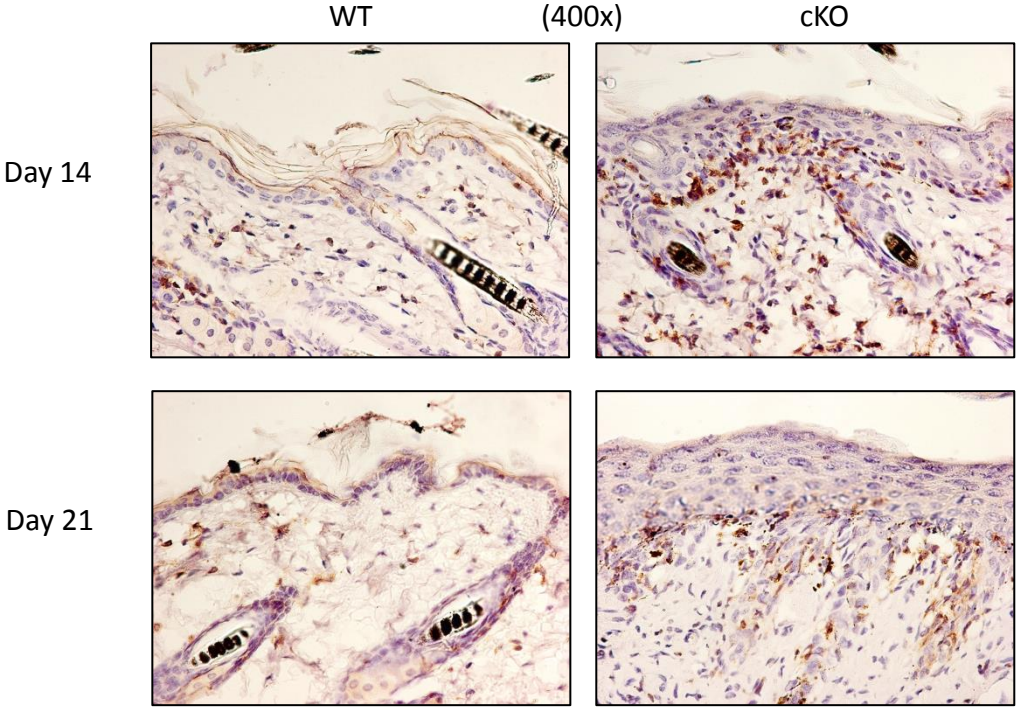

Wax Stripping Recovery for 14 and 21 days (CD45 IHC)

Supplemental Figure 4

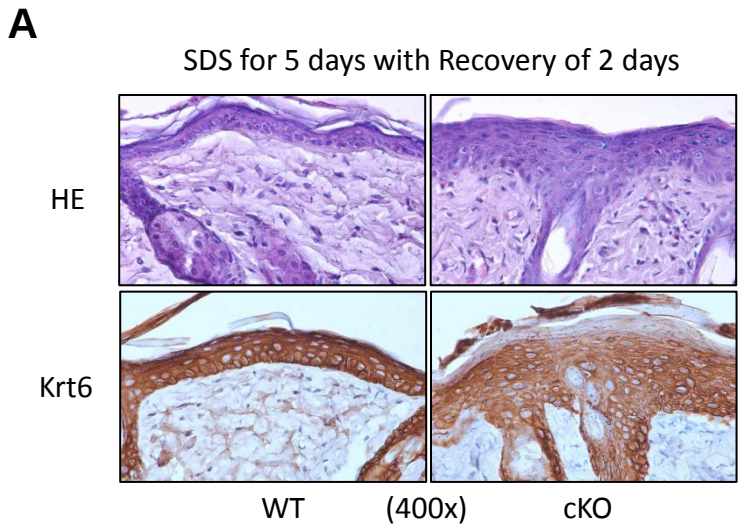

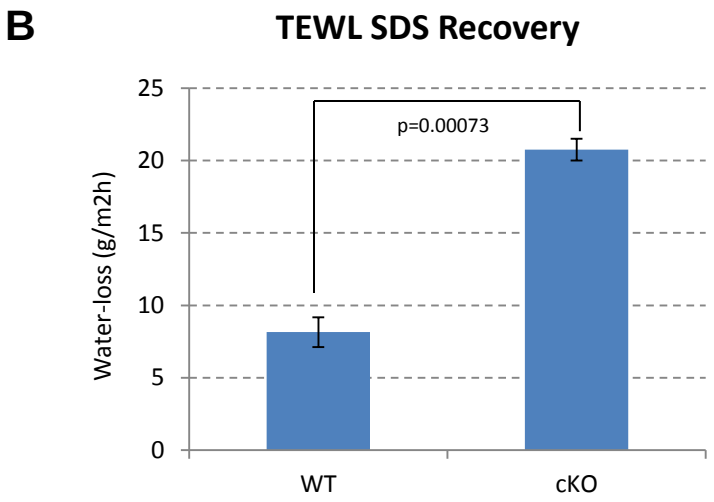

Supplemental Figure 5

A

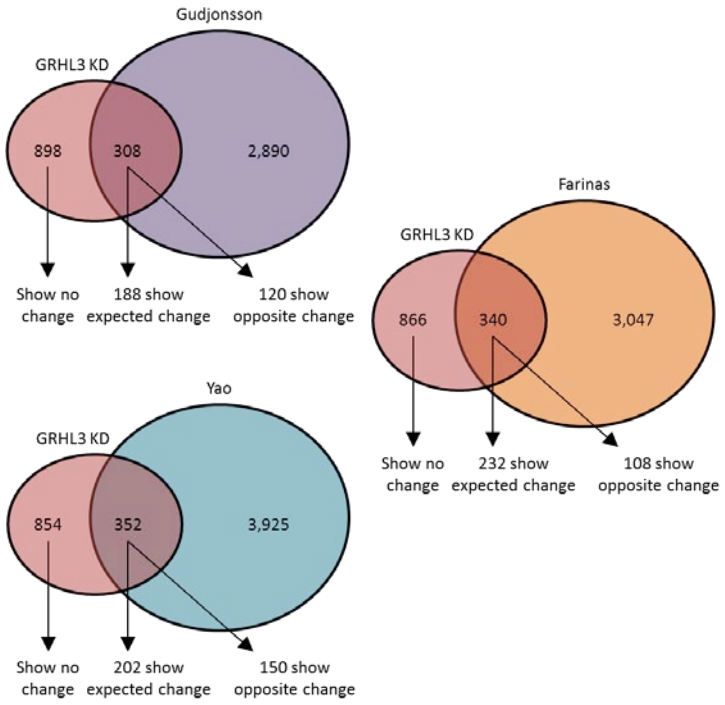

B

Grhl3 Likely ChIP Targets	Expected Direction
Gudjonsson:	78
Yao:	87
Farinas:	100
	Opposite Direction
Gudjonsson:	48
Yao:	63
Farinas:	45
	No Change In Lesions
Gudjonsson:	354
Yao:	329
Farinas:	334

C

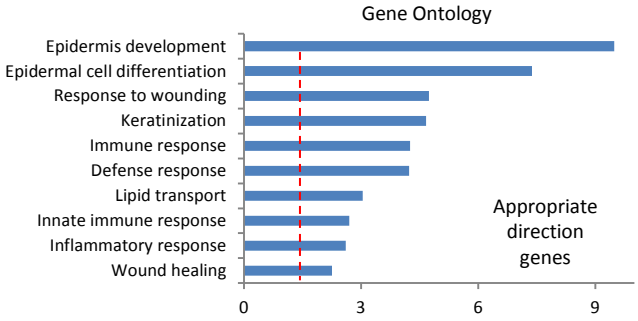

D

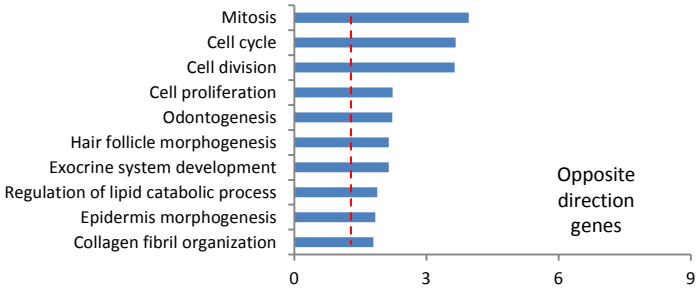

E

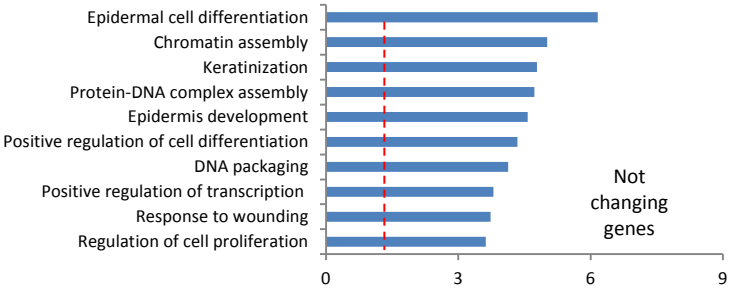

Supplemental Figure 6

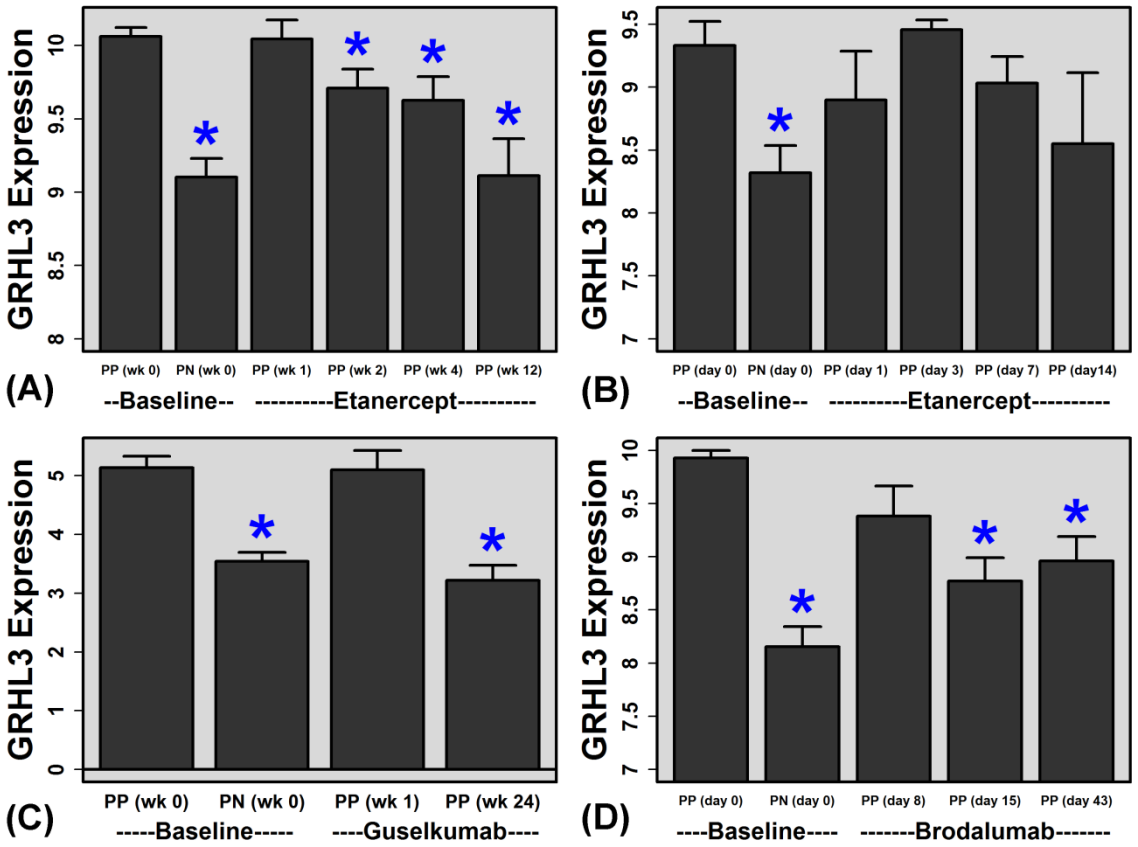

Supplemental Figure 7

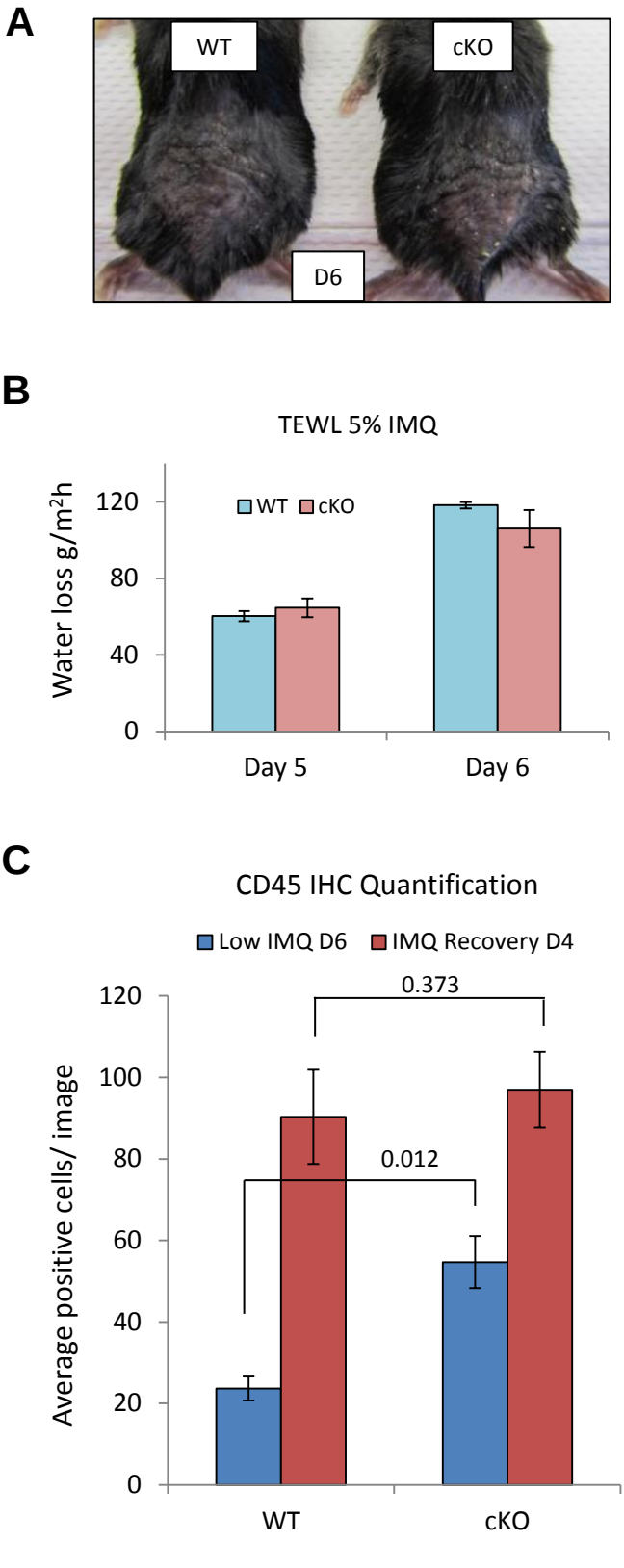

Supplemental Figure 8

A

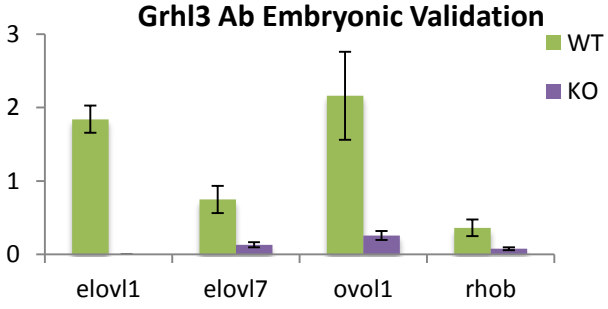

B

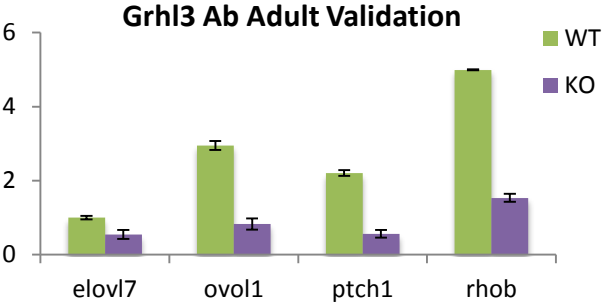

C

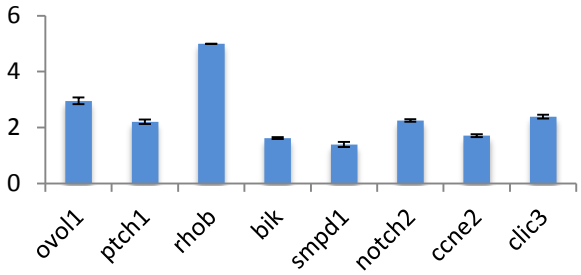

D

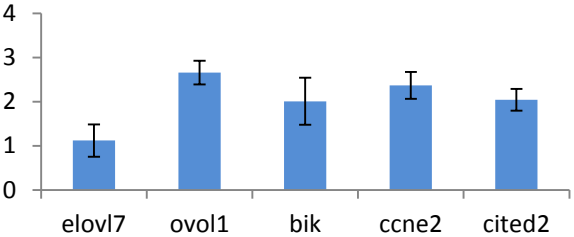

E

	Aligned reads	Peaks FDR <.05
E16.5-1	22952568	11619
E16.5-2	12866522	9685
E16.5 common	---	4035 (42% overlap)
Wax Strip	9437470	4820
IMQ Day 4	80057516	9294

F

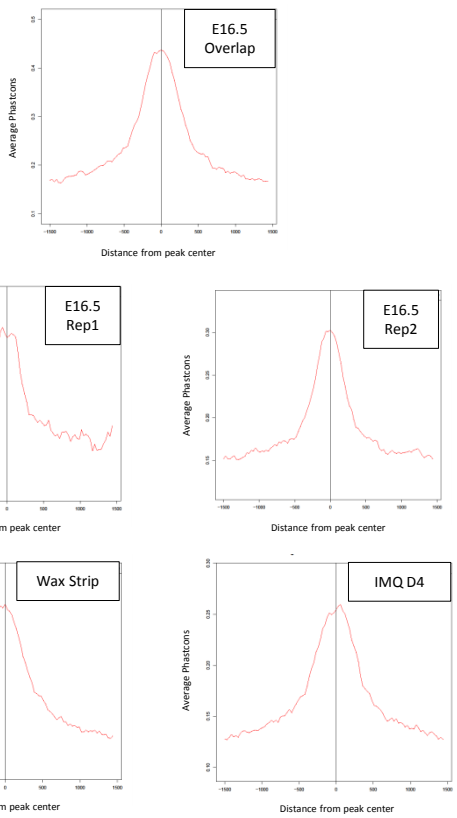

G

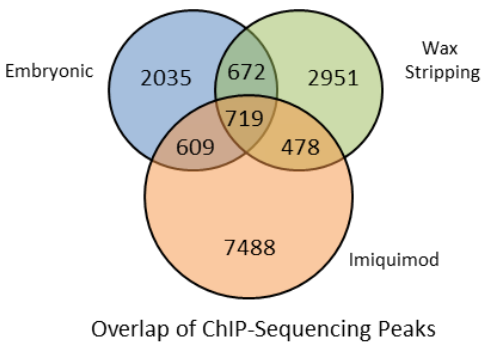

H

	Genome	E16.5	Wax Strip	IMQ
Peaks	NA	4035	4820	7974
Grhl3 Cons	9928	168	118	118
Grhl3 PWM	3,421,980	620	477	686

Supplemental Figure 9

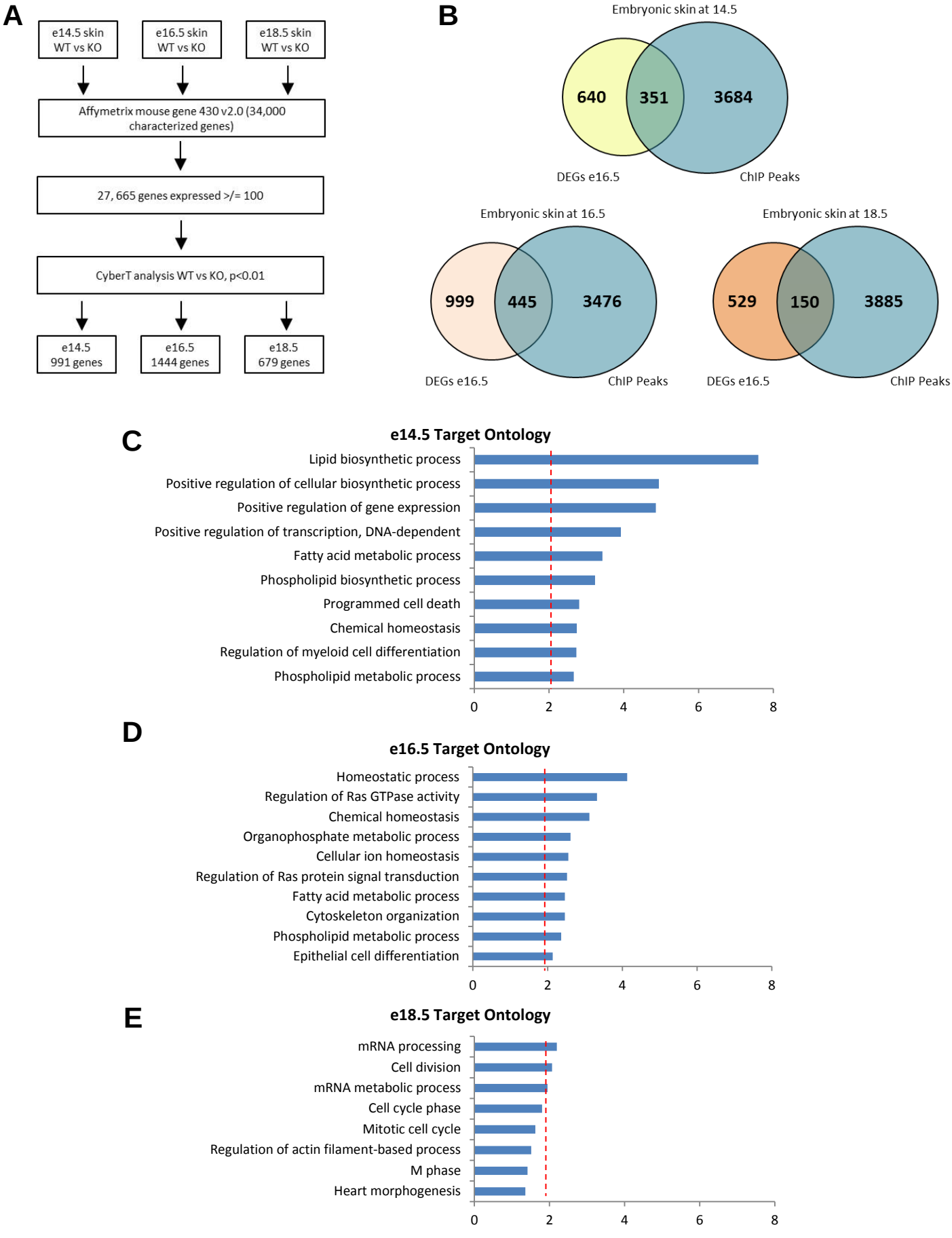

Supplemental Figure 10

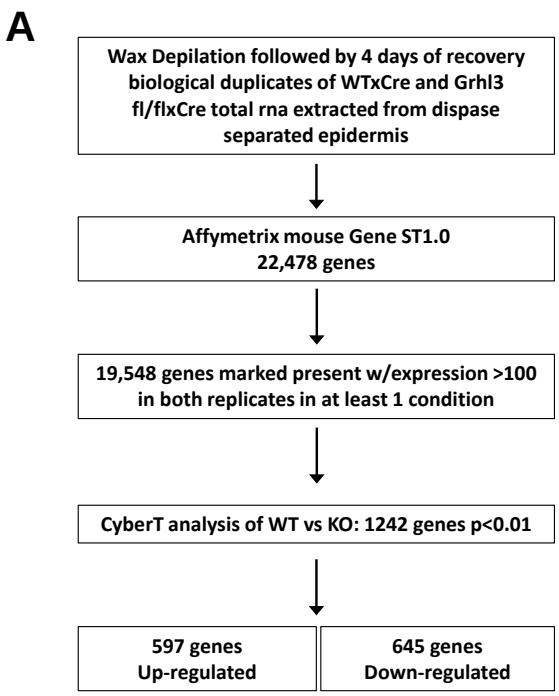

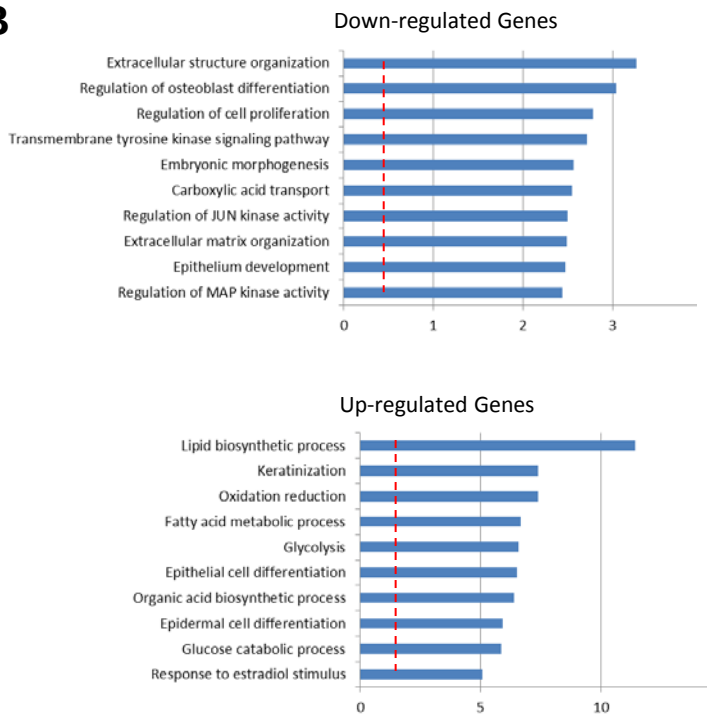

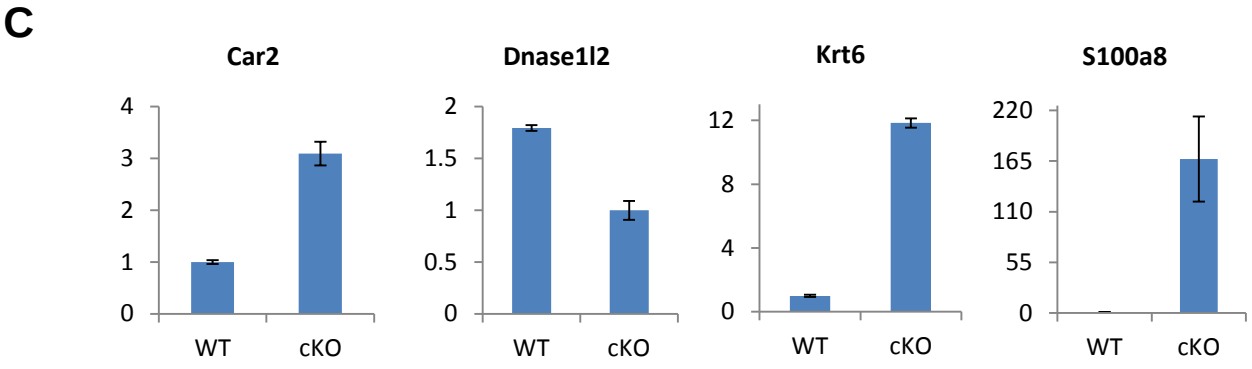

Supplemental Figure 11

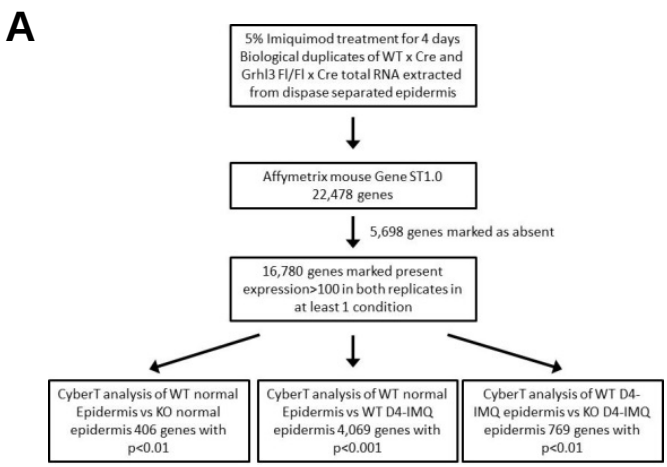

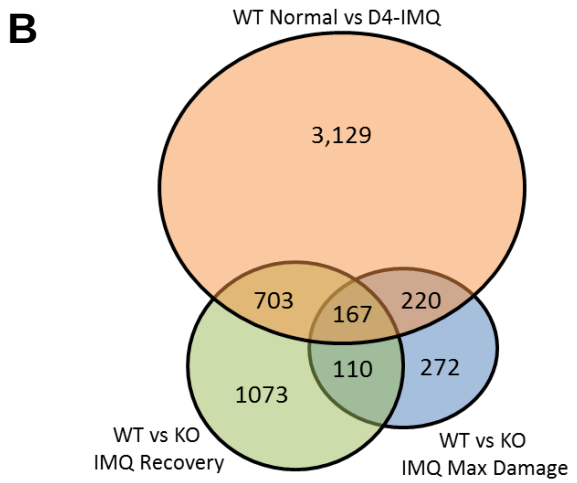

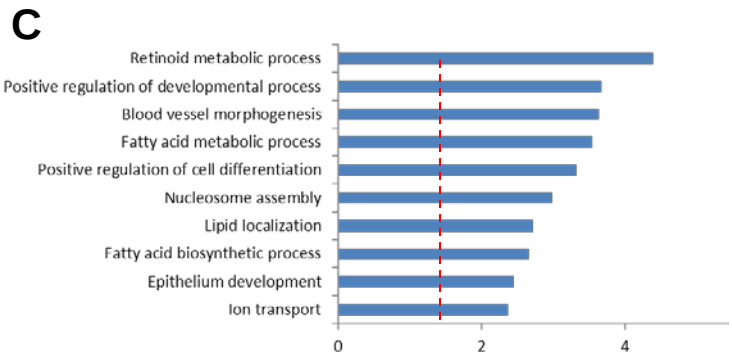

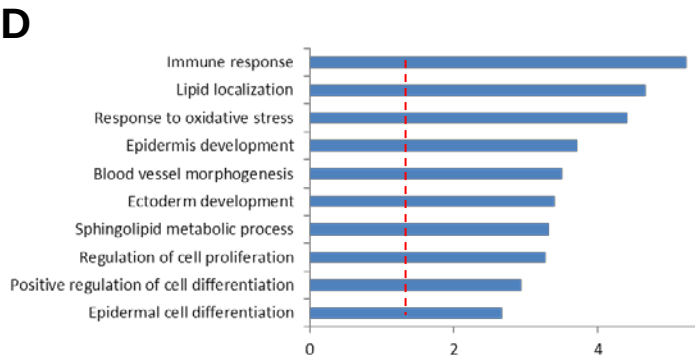

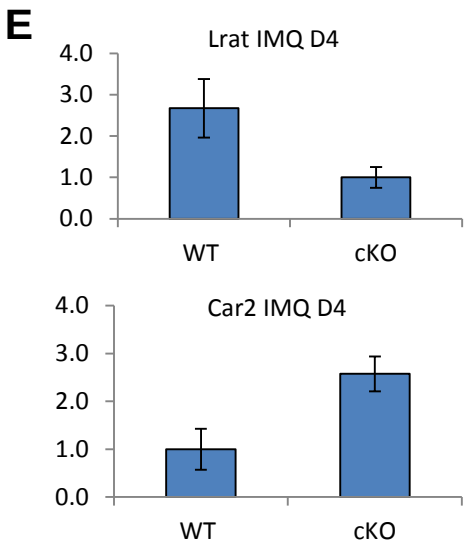

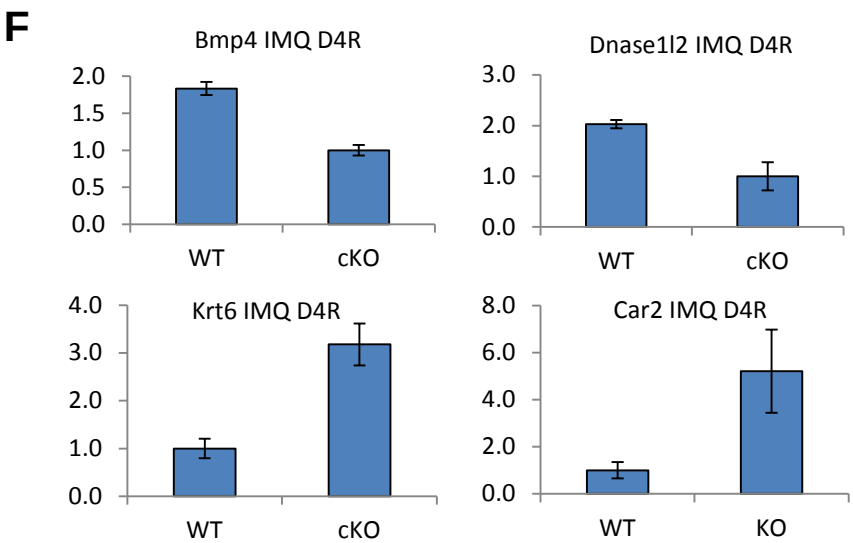

Supplemental Figure 12

A

Embryonic direct targets

Structural proteins: Lor, Evpl, and Ppl

Epithelial differentiation: Foxq1, Tgm1, Pou2f3, Ptch1, Bmp7, Elf3, Six, Crb3, Pou3f1

Cell death (Cornification): Foxo3, Ppp1r13b, Dnase1l2, Slk, Trp53inp1, Dyrk2, Ncf1, Siva1, Sgpp1, Sod1, Gramd4, Id1

Cell adhesion proteins: Cldn6, Ptprf

Lipid metabolism: Elovl1, Elovl7, Hexb, Smpd1, Smpd3, Tnxb, Abhd5, Sgms1, Mboat2, Agpat3, Plcb3, Faah, Acap1, Pld4, Plbd1, Hadhb, Sgpp1

B

Wax stripping direct targets

Structural proteins: Lor and Ppl

Differentiation related transcription factors: Ovol1, Hoxa5, Notch2, Hes1

Cell death (Cornification): Id3, Trp53inp1, Ppp1r13b, Gadd45b, Dnase1l3, Bnip3, Rhob

Cell adhesion proteins: Pvrl4, Ptprm, Cdon, Dst, Cd36

Lipid metabolism: Smpd1, Agpat5, Plbd1, Tpi1, Elovl3

Wounding and inflammatory response: Stab1, Il17c, Adm

C

Maximum Damage from Imiquimod targets

Epidermal differentiation and barrier related genes

Differentiation related transcription factors: Ovol1 and Gata6

Cell death (cornification): Hdac7 and Prkcb

Cell adhesion proteins: Dsg1b

Lipid metabolism:Pla2g4f, Lpin2, Alox12e, Dhrs9, Acacb, and Elovl3

Epidermal damage response genes

Wounding and inflammatory response:Defb7, Pparg, Tlr3, Stab1, Il1a, Defb3, and Defb14

D

Recovery from Imiquimod targets

Epidermal differentiation and barrier related genes

Differentiation related transcription factors: Ovol1 and Gata6

Cell cycle and proliferation: Ptch1

Cell death (cornification): Shisa5, Rhob, and Jak2

Cell adhesion proteins: Cdh24, Itgb8, Thy1, and Itgb4

Lipid metabolism: Smpd1, Lpin3, Cpt2, Plbd1, and Apoc1

Epidermal damage response genes

Wounding and inflammatory response: Zc3h12a, Il10rb, Il17a, Timp4, Il4ra, Irf6, Stat1, Stab1, Defb3, and Tnfrsf18

E

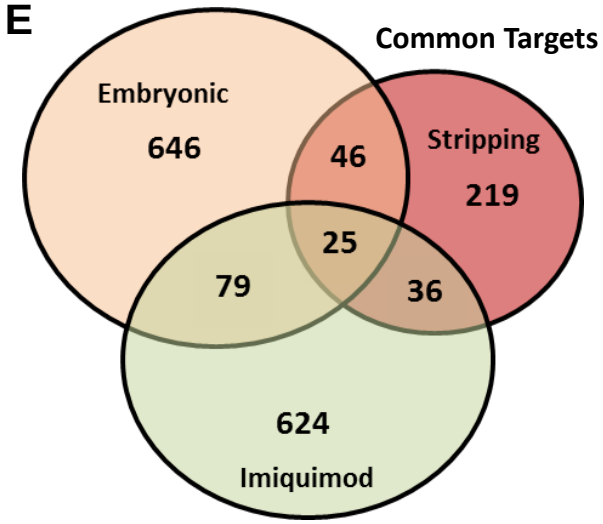

Supplemental Figure 13

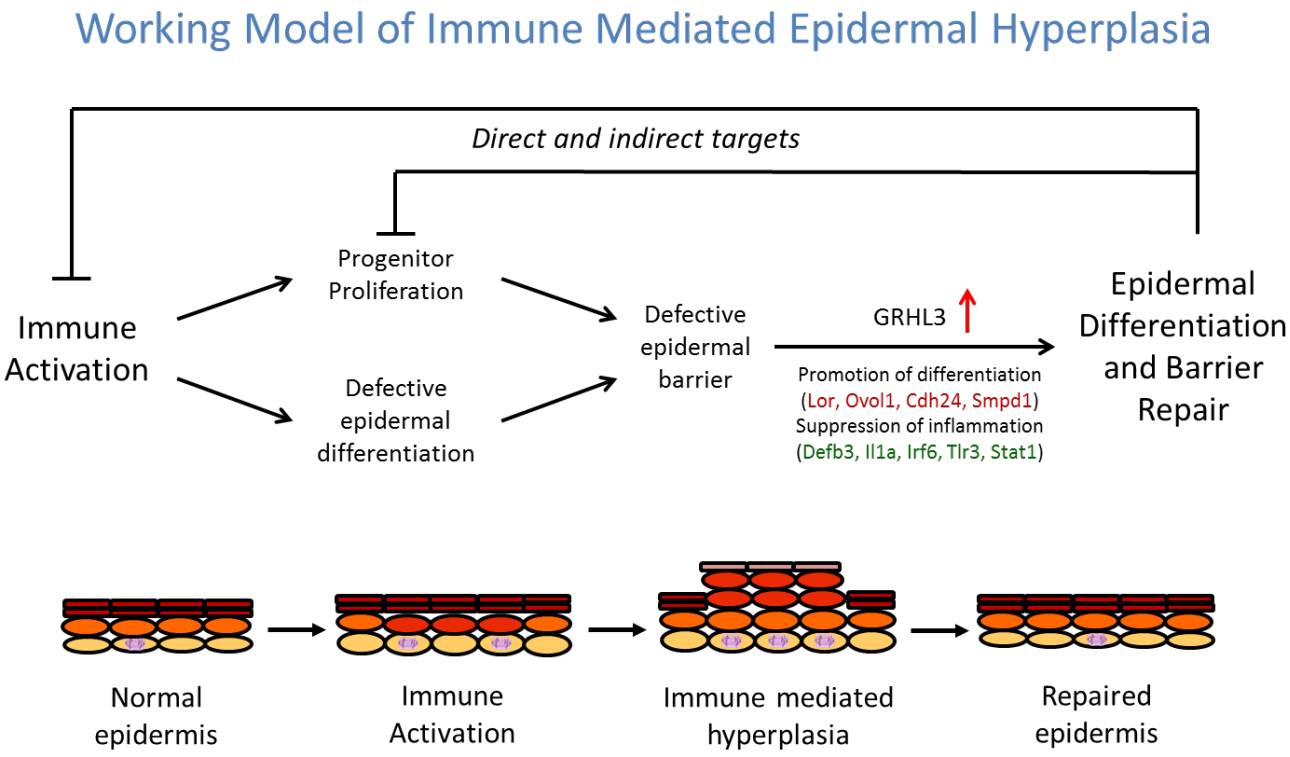

Supplementary Figure Legends

Figure S1. *Grhl3* conditional knockout mice. (a) qPCR of Grhl3 mRNA expression in the epidermis of WT and Grhl3 cKO mice (n=4). (b) Image of wild-type (upper) and cKO (lower) mice at postnatal day 0. cKO pup skin appears less smooth than control littermates and show mild tail and limb abnormalities. (c) Transmission electron microscopy of granular cells at P0 in *Grhl3* WT (left) and cKO (right) epidermis. cKO granular cells do not show the normal flattened morphology seen in control epidermis, continuing to have a more rounded appearance and additionally show accumulation of excess granules. (d) Transmission electron microscopy of differentiated cells at P56 in *Grhl3* WT (left) and cKO (right) epidermis. Adult cKO epidermal cells show a more similar morphology to control cells, having taken on the correct flattened structure and no longer showing excessive granule retention. (e) Trans epidermal water loss measurements in WT and cKO skin in adult 8 week mice (n=4). (f) qPCR of Grh3 altered genes in postnatal day 0 (P0) germline KO, conditional KO (cKO), and postnatal day 56 (P56) conditional KO mice (n=3). Shown is the fold-change in expression in knockout mice relative to WT mice.

Figure S2. Wax stripping epidermal barrier disruption and its repair in mice. (a) TEWL measurements in WT mice after wax stripping (n=2). Maximum TEWL is observed at day 3 after injury followed by a gradual improvement. (b) Quantification of epidermal cell proliferation by BrdU incorporation in WT mice after wax stripping (n=2). Maximum cell proliferation is observed 1 day after injury followed by gradual recovery. (c) Quantification of epidermal thickness in WT mice after wax stripping. Maximum thickness is observed at day 2 after injury followed by gradual normalization.(n=2). (d) IHC of Krt6 in WT epidermis after wax stripping. Krt6 is up-regulated as early as day 1 after injury with maximum expression at day 2, followed by normalization.

Figure S3. Wax stripping recovery is significantly delayed in Grhl3 cKO mice. (a) H&E of back skin at day 14 and 21 of recovery from wax stripping shows continued hyper-thickened epidermis with aberrant cornified structure. (b) IHC of CD45 at day 14 and 21, shows enhanced association of immune cells with the hyper-thickened epidermis of the Grh3 cKO mice during recovery from wax stripping.

Figure S4. SDS-induced epidermal barrier damage recovery is delayed in *Grhl3* cKO mice. (a) H&E and IHC (Krt6) in WT (left panels) and *Grhl3* cKO (Right panels) skin after 5 days of SDS treatment followed by 2 days of recovery. There is increased epidermal hyperplasia in the cKO mice. (b) TEWL in WT and cKO mice after 2 days of recovery from SDS treatment. The cKO mice show increased TEWL.

Figure S5. GRHL3 gene targets in human psoriasis lesional skin. (a) Venn diagrams depicting the overlaps between differentially expressed genes in lesional psoriasis (versus non-lesional skin from three individual human psoriasis microarray datasets [31-33]) and genes differentially expressed after GRHL3 knockdown (KD) in human keratinocytes [35]. (b) Table showing the

number of likely GRHL3 target genes identified from overlapping previous GRHL3 KD data with GRHL3 ChIP-Seq data and differential gene expression in each of the three human psoriasis datasets. (c-e) Gene ontology of the GRHL3 targets going the appropriate direction (c), in the opposite direction (d), or not changing in psoriasis (e).

Figure S6. GRHL3 expression decreases during resolution of psoriatic lesions in response to multiple therapies. (a) Microarray results from Etanercept treatment of psoriasis shows significant decreases in GRHL3 expression at week 2, 4, and 12 after treatment. (b) Microarray results from a second Etanercept study show non-significant trends of reduced GRHL3 expression at day 7 and 14 after treatment. (c) Microarray results from Guselkumab treatment of psoriasis shows significant decreases in GRHL3 expression at week 24 after treatment. (d) Microarray results from Brodalumab treatment of psoriasis shows significant decreases in GRHL3 expression at day 15 and 43 after treatment.

Figure S7. Imiquimod-induced skin abnormalities in WT and *Grhl3* cKO mice. (a) Image of WT and *Grhl3* cKO mice after 6 days of standard (5%) IMQ treatment. Inflamed thickened skin with redness is observed in mice of both genotypes. (b) TEWL in WT and cKO mice at Day 5 and 6 of 5% IMQ treatment. TEWL is similar in mice of both genotypes. (c) Quantification of CD45 positive cells in the dermis of WT and cKO mice at day 6 of 0.25% IMQ treatment and at recovery day 4 of 5% IMQ treatment (N=2 for WT and cKO, multiple 40x images for each replicate where counted in a blind manner). With low dose IMQ treatment there are increased numbers of CD45-positive cells in the skin of cKO mice.

Figure S8. Validation of the GRHL3 Antibody and analysis of GRHL3 ChIP-seq peaks. (a) ChIP-PCR validation of the GRHL3 antibody using chromatin from e18.5 embryonic skin. Known GRHL3 targets are precipitated from WT skin but not *Grhl3* gene-deleted skin (n=2). (b) ChIP-PCR validation of the GRHL3 antibody using chromatin from adult skin. Known GRHL3 targets are precipitated from WT skin but not *Grhl3* gene-deleted skin (n=2). (c) ChIP-PCR validation of GRHL3 peaks in wax stripped adult skin (n=2). The y-axes in panels a-e represent normalized percent of input. (d) ChIP-PCR validation of GRHL3 peaks in IMQ-treated adult skin (n=2). (e) Chart depicting the number of aligned reads and called GRHL3 peaks in the GRHL3 ChIP-seq experiments. (f) Phastcon charts showing the sequence conservation within the GRHL3 peaks in each of the ChIP-seq experiments and the overlap of the two independent embryonic experiments. (g) Venn diagram depicting the overlap in GRHL3 ChIP-seq peaks between all three experiments. (h) Chart depicting the number of GRHL3 perfect consensus and PWM sites genome wide versus the number observed in our ChIP-seq data.

Figure S9. Embryonic gene expression analysis in *Grhl3* gene-deleted skin. (a) A flow chart depicting microarray analysis of Affymetrix mouse 430 v2.0 gene expression arrays in embryonic skin from three different developmental time points (WT and *Grhl3* KO). (b) Venn diagrams showing the individual overlaps between differentially expressed genes (DEG) in Grhl3 KO skin from e14.5, e16.5 and e18.5 with e16.5 GRHL3 ChIP-Seq peaks. (c-e) Top gene

ontology categories using DAVID in embryonic skin for the individual overlaps at e14.5 (c), e16.5 (d), and e18.5 (e).

Figure S10. Differentially expressed genes in *Grhl3* cKO skin after wax stripping. (a) Flow chart depicting microarray analysis of Affymetrix mouse ST1.0 gene expression arrays after wax stripping in control and cKO mice. (b) Top gene ontology categories for the up- and down-regulated genes in cKO skin after wax stripping. (c) qPCR validation of the changes in mRNA levels for selected Grhl3 regulated genes after wax stripping (n=3).

Figure S11. Differentially expressed genes in Grhl3 cKO skin after Imiquimod treatment. a) Flow chart depicting microarray analysis of Affymetrix mouse ST1.0 gene expression arrays after IMQ treatment in control and cKO mice. (b) Venn diagram depicting the overlap between i) the wild-type epidermal response to IMQ treatment (WT normal vs Day 4 of IMQ treatment), ii) the differentially expressed genes in *Grh3* cKO epidermis at Day 4 of IMQ (WT vs KO IMQ Max Damage), and iii) the differentially expressed gene in cKO epidermis at day 4 of recovery from IMQ (WT vs KO IMQ Recovery). (c) Top gene ontology categories for DEGs genes between WT and cKO at day 4 of 5% IMQ treatment. (d) Top gene ontology categories for DEGs genes between WT and cKO at recovery day 4 from 5% IMQ treatment. (e-f) qPCR validation of selected Grhl3 regulated genes at day 4 of 5% IMQ (e) and recovery day 4 from 5% IMQ (f) (n=3).

Figure S12. Proposed direct GRHL3 targets in embryonic epidermis and after injury recovery from wax stripping and IMQ treatment. (a) Likely direct GRHL3 targets and their epidermal related processes during embryogenesis. (b) Likely direct GRHL3 targets and their epidermal related processes after wax stripping. (c-d) Likely direct GRHL3 targets and their epidermal related processes after imiquimod treatment (c) and recovery (d). (e) Venn diagram showing the overlap of likely GRHL3 targets between all three conditions.

Figure S13. Working model for GRHL33 in barrier repair, resolution of hyperplasia, and epidermal differentiation during immune-mediated epidermal injury.